INTERNATIONAL JOURNAL OF ROBUST AND NONLINEAR CONTROL
Int. J. Robust Nonlinear Control **9**, 999–1012 (1999)

DIRECT ADAPTIVE RECONFIGURABLE FLIGHT CONTROL FOR A TAILLESS ADVANCED FIGHTER AIRCRAFT

KEVIN A. WISE[1]*, JOSEPH S. BRINKER[1], ANTHONY J. CALISE[2], DALE F. ENNS[3], MICHAEL R. ELGERSMA[3] AND PETROS VOULGARIS[4]

[1]*The Boeing Company, Phantom Works Division, P.O. Box 516, St Louis, MO 63166-0516, U.S.A.*
[2]*Georgia Institute of Technology, School of Aerospace Engineering, 270 Ferst Drive, Atlanta, GA 30332-0150, U.S.A.*
[3]*Honeywell Technology Center, 3660 Technology Drive, Minneapolis, MN 55418, U.S.A.*
[4]*University of Illinois Urbana–Champaign, Decision and Control Laboratory, 1308 West Main St., Urbana, IL 61801-2307, U.S.A.*

SUMMARY

This paper presents a direct adaptive reconfigurable flight control approach and demonstrates its effectiveness via an application to an advanced tailless fighter aircraft. The reconfigurable control law is based on a dynamic inversion controller in an explicit model following architecture. An on-line neural network is used to adaptively regulate the error between the desired response model and the actual vehicle response. An on-line control allocation scheme generates individual control effector commands to yield the moments commanded by the controller, while prioritizing critical axes and optimizing performance objectives such as maneuver load alleviation. An on-line system identification module generates estimates of the vehicle's stability and control derivatives for use in control allocation and command limiting. The reconfigurable control laws are demonstrated by comparing their performance to a dynamic inversion control law when unknown failure/damage are induced. Copyright © 1999 John Wiley & Sons, Ltd.

Key words: tailless fighter aircraft; reconfigurable flight control; adaptive neural networks; system identification; control allocation

INTRODUCTION

Reconfigurable flight control refers to the ability of a control system to adapt to unknown failures and damage. This expands on the capability of many currently fielded systems (e.g. F/A-18), where the control laws adapt to failures identified by the failure detection and isolation (FDI) algorithms to provide safe operation and desirable handling qualities. Undetectable failures and damage are accommodated only through the inherent robustness of the control laws with no guarantees of stability or good handling qualities. As a result, reconfigurable control laws offer obvious enhancements in flight safety and mission effectiveness.

Reconfigurable flight control has received considerable attention in recent literature, and several approaches have been proposed. The self-repairing flight control system[1] achieved failure

* Correspondence to: Kevin A. Wise, The Boeing Company, Phantom Works Division, P.O. Box 516, St Louis, MO 63166-0516, U.S.A.

CCC 1049-8923/99/140999–14$17.50

and damage tolerance through a reconfigurable flight control system which performed on-line damage isolation and estimation using hypothesis testing techniques in conjunction with a bank of Kalman filters. Response characteristics were compared to a nominal model to isolate failures and estimate the control derivatives of the failed/damaged surface for use in a pseudoinverse control allocation scheme. This work was extended by Chandler *et al.*,[2] where a Hopfield network was used to generate an optimal model following control based on stability and control derivative estimates from an on-line least-squares system identification algorithm. The self-designing controller[3] program successfully flight-tested a scheme on the VISTA/F-16 aircraft which used least-squares system identification, with spatial and temporal constraints, to estimate the stability and control derivatives required for the solution of a receding horizon optimal control problem. Pachter *et al.*,[4] employed a similar approach to maximize an aircraft's tracking performance before and after control surface failures, while preventing instability and departure. Kim and Calise[5] presented an approach based on neural networks for a feedback linearization control architecture and demonstrated the approach via simulation studies with an F/A-18 aircraft. Approaches based on genetic algorithms,[6] a linear model following architecture which minimizes the upper bound of the tracking error,[7] and sliding modes[8] have also been proposed.

Significant research has also been performed in the areas of system identification and control allocation, which directly support reconfigurable control. Chandler *et al.*[9] developed a static system identification scheme based on least-squares estimation which incorporates *a priori* information to enhance parameter estimates. Windowing techniques are used to produce accurate parameter estimates during normal operation and following abrupt changes to the aircraft (e.g. failures or damage). The estimation algorithm is disabled during periods of low excitation to prevent the generation of erroneous estimates. Carrette *et al.*[10] propose the use of a data selection criterion, based on singular value decomposition techniques, that discards the poorly informative data in order to decrease the total mean square error of the estimated parameters. Pan and Basar[11] have proposed an alternate method which estimates uncertain parameters based on H_∞ control and filtering methods.

A variety of approaches have also been proposed for on-line control allocation. Durham and Bordignon[12] limit the moment commands to the attainable moment rate subset, which is the set of moments which can be generated by the control effector suite subject to position and rate limit constraints. Pseudoinverse control allocation was employed by Huang[13] to implement the control distributor concept. Buffington[14] has developed a control allocation approach for dynamic inversion control laws which decomposes the control law into a sequence of prioritized portions and scales these portions to provide command limiting which prevents actuator saturation and yields graceful response degradation for unachievable commands.

Our reconfigurable flight control approach is based on a dynamic inversion control law in an explicit model following framework. The dynamic inversion[15–17] architecture was selected since it is commonly used for aircraft flight control design. Dynamic inversion offers inherent gain scheduling to accommodate non-linear dynamics and direct tuning of flying qualities parameters through the desired dynamics.

An on-line neural network, based on the work of Kim and Calise,[5] is used to adaptively regulate the error in the plant inversion. This network stabilizes the system following failures or damage, thus reducing the criticality of system identification. On-line control allocation is used to generate individual control effector commands which yield the desired rotational accelerations while optimizing performance objectives such as maneuver load alleviation and radar signature. On-line system identification is used to estimate the control derivatives used by the control

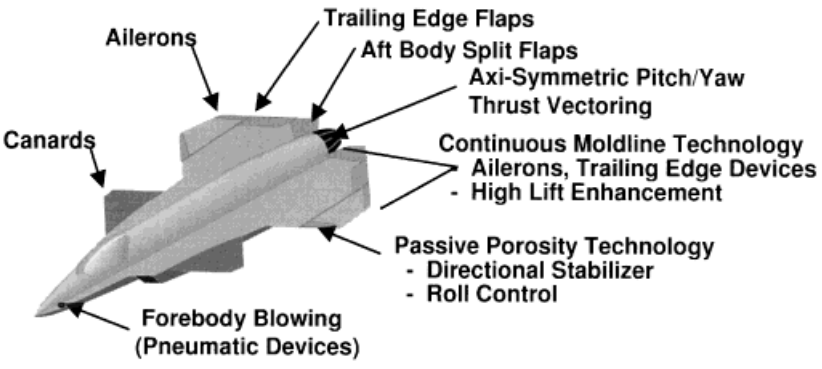

Figure 1. Tailless advanced fighter aircraft (TAFA)

allocation algorithms. This reconfigurable control law is demonstrated via an application to the Boeing tailless advanced fighter aircraft (TAFA),[18] shown in Figure 1.

This paper presents an overview of the TAFA aircraft and its critical failure and damage modes. Reconfigurable control laws using the direct adaptive control architecture are developed for the TAFA vehicle and evaluated at several key operating conditions. Additional details on the models, flight control system design, and analysis are provided in Boeing's RESTORE system design report.[19]

TAFA AIRCRAFT DESCRIPTION

The TAFA aircraft is a conceptual design of an advanced fighter configuration which blends an extensive suite of conventional and innovative control effectors to achieve high agility in a low observable design. The TAFA is a single engine, single seat fighter designed for air-to-air and/or air-to-ground missions.

The TAFA airframe is characterized by a chined forebody, symmetric air inlets, and no vertical tail. The wing and all moving canard are thin and feature a moderate aft sweep and no dihedral. The leading edge of the wing is equipped with passive porosity which can be used as a low rate roll control device during covert maneuvers.

The trailing edge of the wing features ailerons, trailing edge flaps and aft body split flaps. The trailing edge flaps provide a powerful pitch control effector which can also be deflected differentially to augment the ailerons during rolling maneuvers. If necessary, the flaps and ailerons can be deflected in opposing directions to generate yawing moments without inducing roll. The aft body split flaps are 'clamshell' devices which consist of two panels on each side of the aircraft. One panel opens above the wing and the other below the wing to produce yawing moments while inducing very little roll. The all moving canards are used as a low-rate trim device for performance optimization, but also provide supplementary yaw control power through differential deflections. In addition, the canards generate substantial nose down control capability to help meet control margin requirements at high angles of attack.

The TAFA is powered by a moderate bypass ratio turbofan engine equipped with axi-symmetric thrust vectoring. The pitch and yaw thrust vectoring enhance maneuvering capabilities and stability augmentation. In addition, main engine thrust is routed to forebody ports for pneumatic control. The ports are mounted to serve as a yaw control device.

The mission scenarios and critical maneuvers for evaluating the reconfigurable control laws are based on requirements for a low-signature, Class-IV light-attack or strike-fighter aircraft, and were selected from the mission profile of Figure 2. Powered approach, air combat maneuvering, low altitude ingress/egress, and high-speed supercruise mission segements were selected. The maneuvers performed during these mission phases have been selected to fully utilize the available control power of the aircraft and to provide sufficient challenge for the system identification, reconfiguration, and control allocation algorithms.

The reconfigurable control laws must provide stability and good handling qualities during normal operation, as well as under failures and damage. The failure modes are classified, depending on the severity of the failure or damage, as Class 1 (C1) and Class 2 (C2), and correspond to the requirement to meet Level 2 or 3 flying qualities. These classifications correspond very closely to the operational states II and III defined in MIL-F-9490D. Class 1 incidents include either minor damage or single failures, where the actuator/control effector responds to the failure as designed. Several examples are (1) ratcheting of the surface to a zero position, (2) 'floating' in a damped-trail mode, or (3) locking at the deflection where failure occurred. Also included are minor damage scenarios which result in partial (physical) loss of a control effector.

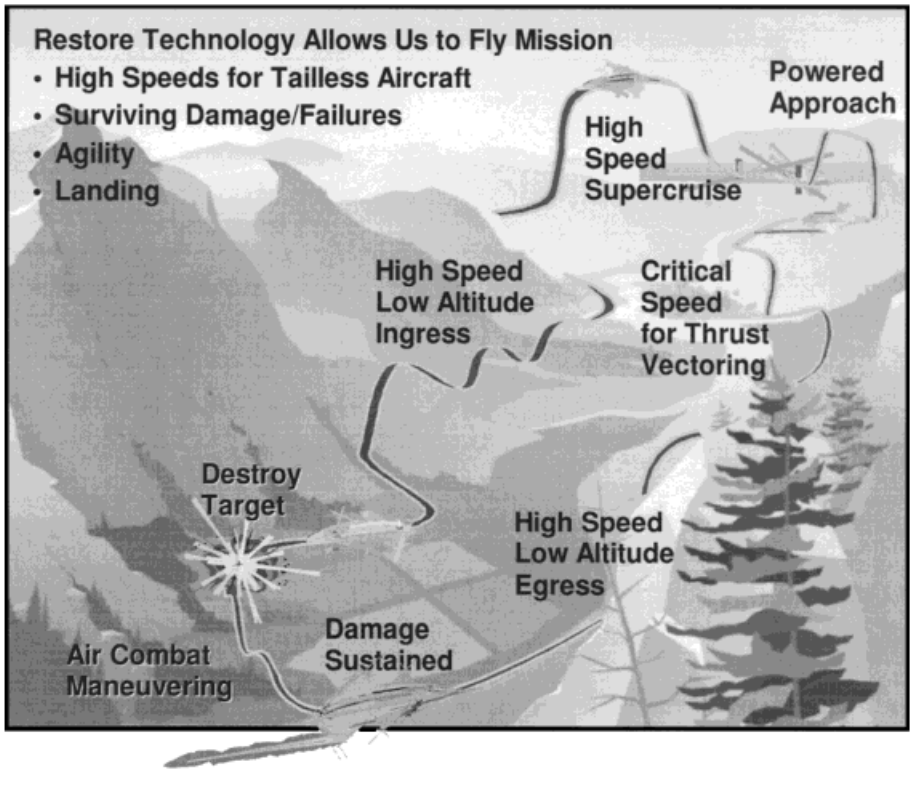

Figure 2. RESTORE mission profile

Class 2 includes any combination of two Class 1 incidents, plus situations in which the actuator is unable to respond to the failure as designed. Hard-over failure of an effector to its maximum position, for example, will likely require constant use of a comparable surface for trim alone, effectively disabling two effectors. Likewise, complete loss of a large all-moving surface (e.g. trailing edge flap) is a significant damage state, and may also be evaluated under the less severe flying qualities requirements.

The large control effector suite of the TAFA aircraft results in a large number of potential failure and damage conditions.[18] In order to streamline verification and validation of the reconfigurable control laws, an effort was performed to identify the critical failure and damage conditions at each of the flight conditions. These critical failure and damage conditions are the primary conditions used to evaluate the performance of the reconfigurable control laws. Selection of the critical failure and damage conditions was based on an achievable dynamics analysis[18] of candidate failure/damage configurations. Classes 1 and 2 conditions which allowed the flying qualities objectives (Level 2 for C1 failure and Level 3 for C2 failure) to be met through optimal use of the remaining control effectors were selected for subsequent analysis. The critical failure and damage conditions are tabulated along with the vehicle's static stability characteristics under these conditions in Figure 3.

RECONFIGURABLE CONTROL LAWS

The proposed reconfigurable control law architecture is shown in Figure 4. It is based on a dynamic inversion control law in an explicit model following framework.

The on-line neural network adaptively regulates the inversion error between the plant model assumed by the control law and the true aircraft. Inversion errors may be due to modelling uncertainties, or induced by failures/damage. The neural network detects that an inversion error is present by monitoring the tracking error between a desired response model and the true aircraft. Large errors will cause the network to augment the desired dynamics input to the inverting controller with a signal which attempts to cancel the inversion error. The neural network has the ability to stabilize the vehicle following failures/damage without requiring system identification estimates of the stability and control derivatives. This reduces the criticality of system identification in the overall reconfigurable control law. The neural network's stabilizing characteristics are supported by an analytical proof of stability. Details of the neural network controller and performance results are provided by Calise *et al.*[20]

The neural controller models the inversion error using a basis function expansion implemented via a sigma-pi neural network. The network weights are updated on-line (no pre-training of the network) using a weight adaptation law derived from Lyapunov stability theory.

Figure 5 illustrates the roll channel control law architecture, which incorporates the desired response model, the inverting controller ($\hat{f}^{-1}$), and the on-line neural network. The flying qualities requirement in the roll axis is a first-order stability axis roll rate (p_s) response given by

$$\frac{p_s}{p_{sc}} = \frac{1}{\tau_R s + 1}$$

which is selected as the desired response model. The resulting pseudocontrol input to the inverting controller is

$$u_p(t) = K_p \tilde{p}(t) + \dot{p}_{cf}(t) - \hat{u}_{ad_p}(t)$$

Mission Phase	Flight Condition	Maneuvers	Notes
Powered Approach (PA)	V = 150 KTS h = Sea Level AOA = AOA(@1g)	• Offset Approach • Straight Approach • Field Landing	• Level 1 FQ Req. • Level 2 FQ Req. • Level 3 FQ Req.
Air Combat Maneuvering	V = 0.6 M h = 15Kft AOA = AOA(@3-5g)	• High-AOA Acquisition • High-AOA Tracking	Critical M/Alt for TVC Based On ACONTA Study
Ingress/Egress	V = 0.9 M h = Sea Level AOA = AOA(@1g)	• Ground Target Acquisition • TAP	
High-Speed Supercruise	V = 1.4 M h = 22.5Kft AOA = AOA(@1g) qbar = 1200 psf	• Turbulent-Air Penetration (TAP)	

Flight Condition	Critical Failure / Damage Modes	Time to Double ~ sec (Pitch / Yaw)
Powered Approach	C1: Floating Aileron C2: Vectoring Nozzle & Single Aft Body Flap Locked to 0°	(Stable / 0.9 sec) (Stable / 0.9 sec)
Air Combat	C1: Trailing Edge Flap Locked to 0° C2: Vectoring Nozzle Locked to 10°,10°	(0.8 sec / 0.45 sec) (0.8 sec / 0.45 sec)
Ingress/Egress	C1: Nozzle Disabled C2: Missing Trailing Edge Flap	(0.17 sec / 0.21 sec) (0.14 sec / 0.21 sec)
Supercruise	C1: Trailing Edge Flap Locked at 0° C2: Missing Aft Body Flap	(0.17 sec / 0.21 sec) (0.14 sec / 0.21 sec)

Figure 3. Critical C1 and C2 failures for each mission segment

where $u_p(t)$ is the roll channel pseudocontrol, $\hat{u}_{ad_p}(t)$ is the roll channel adaptation signal (output of the neural network), and $\dot{p}_{cf}$ is the filtered stability axis roll acceleration. For a linearly parameterized network, the network output is defined by

$$\hat{u}_{ad_p}(t) = \sum_{j=1}^{N} \hat{w}_{pj}\xi_{pj} = \hat{w}_p^T\xi_p$$

where ξ_p are the basis functions of the network, and $\hat{w}_p \in R^N$ is its weighting vector. The weight update law is given by

$$\dot{\hat{w}}_p = -\gamma_p[\tilde{p}\xi_p + \eta|\tilde{p}|\hat{w}_p]$$

The learning rate (γ_p) was selected as 20 for this application.

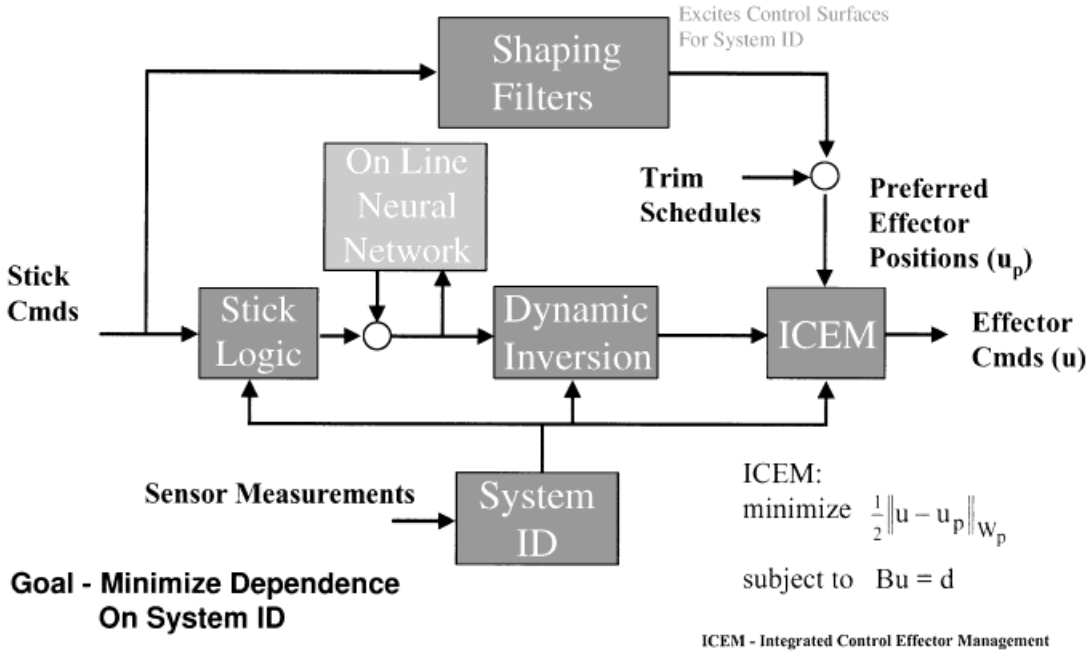

Figure 4. Reconfigurable control law architecture

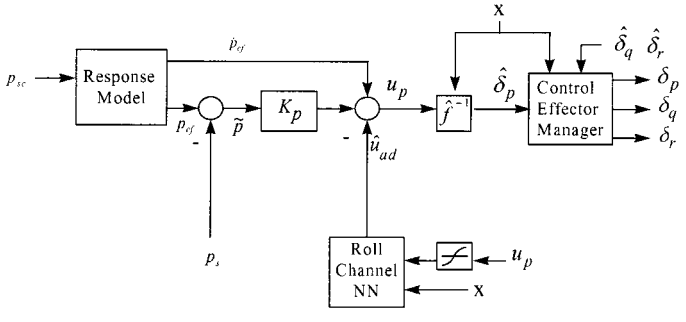

Figure 5. Structure of roll channel adaptive controller

The roll neural network is linear in sideslip, roll rate and yaw rate, and quadratic in angle of attack and the roll channel pseudocontrol. The pseudocontrol inputs to the network are passed through a sigmoidal activation function, $\sigma(u_p)$, to guarantee the existence of a fixed-point solution (required for the analytical proof of stability). The basis functions of the network (ξ_i) comprised the various combinations of products formed from the network's parameterizing variables. The network output is then formed as the sum of the products of the basis functions and their respective network weights. The roll neural network architecture is illustrated in Figure 6.

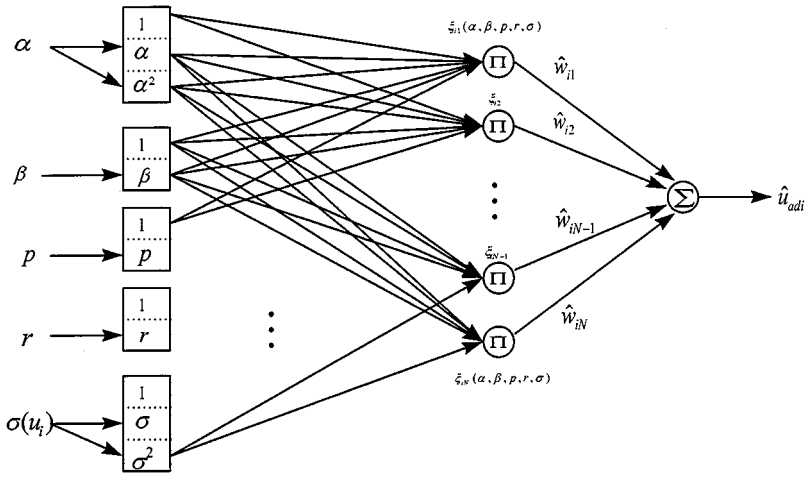

Figure 6. Structure of roll channel neural network

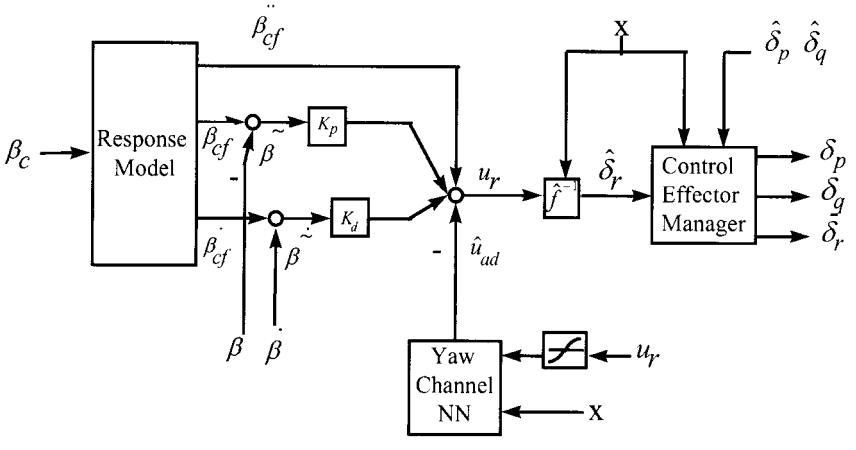

Figure 7. Structure of yaw channel adaptive controller

The flying qualitites requirements in the pitch and yaw axes are specified by the second-order transfer functions

$$\frac{x}{x_c} = \frac{\omega_n^2}{s^2 + 2\zeta_n\omega_n s + \omega_n^2} \quad \begin{array}{l} \text{Pitch: } x = \alpha,\ \omega_n = \omega_{sp},\ \zeta_n = \zeta_{sp} \\ \text{Yaw: } x = \beta,\ \omega_n = \omega_{dr},\ \zeta_n = \zeta_{dr} \end{array}$$

Since both axes use second-order response models, the adaptive control architecture will be the same for these axes. This architecture is shown for the yaw channel in Figure 7. The network

weights are adapted using the law

$$\dot{\hat{w}}_i = -\gamma_i[e_i^{\mathrm{T}} P_i \mathrm{b} \xi_i + \eta |e_i| \hat{w}_i]$$

where $e_i = [\tilde{x} \ \dot{\tilde{x}}]^{\mathrm{T}}$, $b = [0 \ 1]^{\mathrm{T}}$, and

$$P_i = \begin{bmatrix} \dfrac{k_{d_i}}{2k_{p_i}} + \dfrac{k_{p_i}}{2k_{d_i}}\left(1 + \dfrac{1}{k_{p_i}}\right) & \dfrac{1}{2k_{p_i}} \\ \dfrac{1}{2k_{p_i}} & \dfrac{1}{2k_{d_i}}\left(1 + \dfrac{1}{k_{p_i}}\right) \end{bmatrix}$$

The learning rates were selected to be $\gamma_\alpha = 20$ in the pitch axis and $\gamma_\beta = 20$ in the yaw axis.

The yaw neural network parameterization is identical to the roll channel. The pitch channel neural network is linearly parameterized with pitch rate and quadratically parameterized with angle of attack and the pitch pseudocontrol.

The integrated control effector management (ICEM) algorithm performs control allocation while optimizing selected performance objectives. It accepts moment commands from the inverting controller (d), control derivatives from the system identification algorithm (B matrix), and the available control deflections as inputs to generate the individual control effector commands (u). If the moment commands can not be satisfied, the weighted error norm, $\frac{1}{2}\|Bu - d\|_{W_d}$, is minimized. The weighting matrix, W_d, is used for axis prioritization by heavily weighting the errors in the critical axes. When the moment commands can be satisfied, the redundancy in the control effector suite is used to satisfy the moment commands while driving the effectors toward a preferred position (u_{p}).This notion is made precise with the objective to minimize

$$\tfrac{1}{2}(u - u_{\mathrm{p}})^{\mathrm{T}} W_{\mathrm{p}} (u - u_{\mathrm{p}}) \text{ where } W_{\mathrm{p}} = W_{\mathrm{p}}^{\mathrm{T}} > 0$$
$$\text{subject to } Bu = d.$$

The control effector preference vector, which comprised trim schedules and signals used to aid identification of the control derivatives, is constrained to lie in the kernel of the B matrix by the control allocation algorithm and thus does not affect the vehicle's response. Quadratic programming algorithms are used to solve the resulting constrained optimization problem. Details of the control allocation algorithms are provided by Enns.[21]

Axis prioritization refers to the desire to give priority to achieving the moments commanded in a given axis when the available control power is insufficient to achieve all commanded moments. Priority is given to axes which are statically unstable to prevent departures, as well as those critical to performing a given task (e.g. pitch axis during terrain following). This priority can be imposed through the control allocation algorithm via the W_d weighting matrix shown above.

Maneuver load alleviation refers to the utilization of the available control effectors in a manner which achieves the desired moments for the vehicle while minimizing the forces or moments (loads) at specified points on the aircraft. Effective load alleviation algorithms can reduce the structural requirements of the aircraft, thereby reducing weight and cost. Maneuverability is maintained by using the effectors in a way which keeps the loads within their acceptable boundaries, while maximizing the control power available to control the aircraft.

Maneuver load alleviation can be achieved using the on-line control alloction algorithms discussed above. The load induced by a given control effector is related to its position (i.e. larger deflections tend to yield larger loads). The preference vector, u_{p}, employed by the control

allocation algorithm can be used to drive the control effectors toward positions which minimize the loads on the aircraft. Since all of the preferred effector positions may not be attainable, the preference weighting matrix is used to assign a relative priority to various effectors being at their preferred position. This matrix reflects the relative influence of the various effectors on the loads to be minimized.

The system identification module uses a least-squares algorithm to estimate the coefficients of a basis function expansion representing the aerodynamic and propulsive forces and moments. These coefficients include the vehicles stability and control derivatives. A singular value decomposition technique is used to eliminate measurements with low information content to prevent erroneous estimates. Filters on the pilot commands are used to generate signals which are added to the control effector preference vector for injection into the kernel of the control distribution matrix. These signals facilitate identification of the control derivatives for surfaces which are ganged together by the control allocation function. This ganging causes the parameters to be colinear, which would normally prevent identification of the individual parameters. The signals in the kernel of the control distribution matrix eliminate this colinearity and allow estimation of the individual parameters. This approach avoids injection of undesirable dither signals when the pilot is not maneuvering the aircraft. In addition, the signals in the kernel of the control distribution matrix can be tied to the magnitude of the pilot input, thereby allowing system identification only during large maneuvers. Details of the system identification algorithms are provided by Elgersma and Enns.[22]

The notation used to describe the aircraft dynamics whose parameters are to be estimated is described below. Let

$$x \in R^n, \quad u \in R^m, \quad H \in R^{n \times k}, \quad b \in R^q, \quad f \in R^n$$

Any dynamical system can be written as the product of a coefficient matrix, H, times a vector of basis functions, $b(x, u)$, plus a residual. The residual can be made arbitrarily small by increasing the number, q, of basis functions. However, this also increases the size of the coefficient matrix, H, which must be recomputed when the system changes (e.g. due to battle damage to an aircraft).To keep the residual small, while using a minimal number of basis functions, a nominal function, $f(x, u)$, which does not depend on any undetermined coefficients can be separated out as shown below.

$$\dot{x} = f(x, u) + H^* b(x, u) + \text{residual}$$

For an aircraft, the aerodynamics forces and moments could be represented by $H*b(x, u)$, while all other terms of the dynamics may be put into $f(x, u)$. This is consistent with the fact that minor damage to the aircraft can significantly change the aero coefficients, while having only a small effect on the mass and moments of inertia.

The system identification approach assumes that x, u, and $\dot{x}$ can be measured with sensors or accurately estimated. Then, by comparing the measured value of $\dot{x}$ with the computed values of $f(x, u)$ and $b(x, u)$, the coefficient matrix H can be computed. For a rigid aircraft, $\dot{x}$ consists of translational acceleration of the e.g. $\dot{v}_{cg} \in R^3$, and angular acceleration $\dot{\omega} \in R^3$. Translational acceleration, $\dot{v}_{cg}$, can be measured with a single 3-axis accelerometer, while rotational accelerations, $\dot{\omega}$, can be computed from measurements of three 3-axis non-collinear accelerometers or estimated by numerical differentiation and filtering of the rotational rates.

After acquiring k samples, let

$$F = [\dot{x}(t_1) - f(x(t_1), u(t_1)), \dot{x}(t_2) - f(x(t_2), u(t_2)), \ldots, \dot{x}(t_k) - f(x(t_k), u(t_k))]$$

and

$$G = [b(x(t_1), u(t_1)), b(x(t_2), u(t_2)), \ldots, b(x(t_k), u(t_k))]$$

The G matrix is size $q \times k$ where $k \gg q$, and thus the equation to solve for H,

$$F = HG$$

represents an over-determined linear algebra problem.

If *a priori* knowledge on the approximate value of H is available, the solution can be biased to stay close to the preferred value, H_0. Let

$$H = H_0 + H_\Delta$$

and combine the last two equations, using a $q \times q$ weighting matrix W, to give

$$[F - H_0 G, 0] = H_\Delta [G, W]$$

The least-squares solution is

$$\begin{aligned} H_\Delta &= [F - H_0 G, 0][G, W]^{\mathrm{T}}([G, W][G, W]^{\mathrm{T}})^{-1} \\ &= (F - H_0 G)\, G^{\mathrm{T}}(GG^{\mathrm{T}} + WW')^{-1} \end{aligned}$$

If the $[G, W]$ matrix is poorly conditioned, its inverse can be approximated using the singular value decomposition:

$$[U_1, U_2]\mathrm{diag}([\Sigma_1, \Sigma_2])[V_1, V_2]^{\mathrm{T}} = \mathrm{svd}([G, W])$$

which yields

$$H_\Delta = [F - H_0 G, 0] V_1 \Sigma_1^{-1} U_1^{\mathrm{T}}$$

SIMULATION RESULTS

Non-linear simulation analysis of the reconfigurable control laws was conducted to test their ability to adapt to critical failure and damage scenarios and evaluate the stability and handling qualities of the vehicle following the critical failures and damage. Simulations were initiated from a trimmed flight condition. Stick or pedal doublets, with a magnitude equal to half of the maximum deflection, were then applied. The failure or damage was introduced 1 s after maneuver initiation. The stick or pedal input was not modified after the failure or damage, thus requiring the reconfigurable control law to stabilize the vehicle (i.e. no pilot aiding to compensate for the failure/damage).

Simulation results are shown for a longitudinal stick input at the ingress/egress flight condition in Figure 8. The simulation results compare the dynamic response of the nominal vehicle (solid line) to that with a missing left trailing edge flap (dotted line). The damage occurs at 2 s (1 s after maneuver initiation).

The first two rows of plots compare the dynamic response parameters for the two conditions. These results show that the reconfigurable control law adapts to the damage and restores the tracking performance in the normal load factor (NL) response. The sideslip excursions caused by the damage are held to less than 4°, while the rotational rates are stabilized.

The final set of plots compare the parameter identification results for the two conditions. These plots show the dimensionalized control derivatives (rotational acceleration per effector

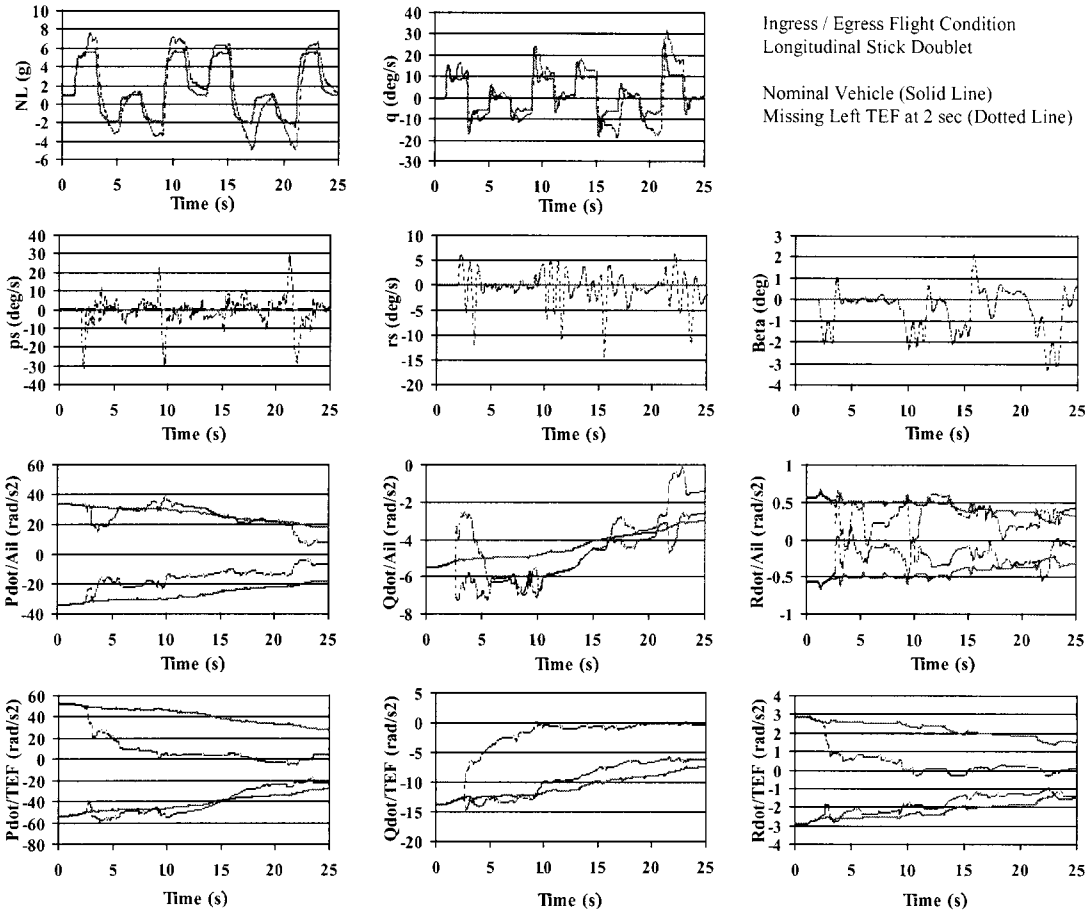

Figure 8. Performance of reconfigurable control law following failure/damage

command) for the ailerons and trailing edge flaps. Control power estimates are generated based on the individual effectors, rather than collective and differential pseudocontrols, to capture the cross axis effects induced by failures and damage. For the failed condition, the left TEF derivatives should go to zero, while the remaining derivatives should be comparable to the nominal case (some differences may be induced due to trajectory deviations and variations in control surface utilization). The results show that the left TEF derivatives tend to zero as expected, while the right TEF derivatives track the nominal values. The damage induces some perturbation in the aileron derivatives prior to the estimates converging to their desired values.

Overall, the responses under the simulated damage condition achieve the goal of providing at least Level 3 flying qualities under severe damage. The responses are stable and the rates adequately damped. More benign maneuvering (which would typically be the case under severe damage) would likely yield improved tracking results.

Good results were obtained for most scenarios (i.e. combinations of flight condition, failures, damage, and pilot inputs). All Class 1 failures/damage were handled very well, with the dynamic

responses being nearly identical to the nominal vehicle. The Class 2 failure/damage scenarios were handled by the reconfigurable control law for most inputs. Failures or damage during aggressive maneuvers can result in control power reductions that prevent stabilization and recovery. Modifying the inputs to aid in recovery from the failure/damage (i.e. pilot aiding in stabilizing the vehicle) may improve results at these conditions.

The benefits on integrating fault detection and identification (FDI) algorithms into the reconfigurable control laws was also investigated via these non-linear simulations. The FDI algorithms were modelled as a fixed time delay in detecting locked or floating control effector failures. The FDI algorithms provided no information about sustained battle damage. The FDI algorithms generated a flag indicating whether an effector was locked or floating. The system ID module uses this flag to remove the failed effector from the regressor matrix, while the control allocation removes the failed effector from the B matrix used to allocate the moment commands. FDI information provided improved performance for locked and floating actuator failures by allowing direct compensation for the failure.

CONCLUSIONS

A reconfigurable control approach has been developed based on direct adaptive control techniques and has demonstrated very good performance in non-linear simulations using tailless advanced fighter aircraft. The direct adaptive approach reduces the criticality of system identification for stabilizing the vehicle following failures and damage, and is supported by an analytical proof of stability. Follow-on research to mature these algorithms includes manned simulation and flight testing.

REFERENCES

1. 'Self-repairing flight control system', *Final Report*, WL-TR-91-3025, Aug 1991.
2. Chandler, P., M. Mears and M. Pachter, 'On-line optimizing networks for reconfigurable control', *Proc.* 32*nd Conf. on Decision and Control*, San Antonio, TX, Dec 1993, pp. 2272–2277.
3. Monaco, J., D. Ward, R. Barron and R. Bird, 'Implementation and flight test assessment of an adaptive, reconfigurable flight control system', *Proc. AIAA GNC Conf.*, New Orleans, LA, Aug 1997, AIAA-97-3738.
4. Patcher, M., P. R. Chandler and M. Mears, 'Reconfigurable tracking control with saturation', *AIAA J. Guidance, Control Dyn.*, **18**(5), 1016–1022 (1995).
5. Kim, B. S. and A. J. Calise, 'Nonlinear flight control using neural networks', *Proc. AIAA GNC Conf.*, Scottsdale, AZ, August 1994, AIAA-94-3646-CP.
6. Baumgarten, G., J. J. Buchholz and W. Heine, 'A new reconfiguration concept for flight control systems', *Proc. AIAA GNC Conf.*, Baltimore, MD, August 1995, AIAA-95-3176-CP.
7. Dhayagude, N. and Z. Gao, 'A novel approach to reconfigurable control systems design', *Proc. AIAA GNC Conf.*, Baltimore, MD, August 1995, AIAA-95-3175-CP.
8. Shtessel, Y. B. and C. H. Tournes, 'Flight control reconfiguration on sliding modes', *Proc. AIAA GNC Conf.*, New Orleans, LA, August 1997, AIAA-97-3632.
9. Chandler, P. R., M. Pachter and M. Mears, 'System identification for adaptive and reconfigurable control', *AIAA J. Guidance Control Dyn.*, **18**(3), 516–524 (1995).
10. Carrette, P., G. Bastin, Y. Genin and M. Gevers, 'Discarding data to perform mode accurate system identification', *Proc. 34th Conf. on Decision and Control*, New Orleans, LA, Dec. 1995, pp. 1823–1824.
11. Pan, Z. and T. Basar, 'Parameter identification for uncertain systems with partial state measurements under an H_∞ criterion', *Proc.* 34*th Conf. on Decision and Control*, New Orleans, LA, Dec. 1995, pp. 709–714.
12. Durham, W. C. and K. A. Bordignon, 'Multiple control effector rate limiting', *AIAA J. Guidance, Control, Dyn.*, **19**(1), 30–37 (1996).
13. Huang, C. Y., 'Analysis and simulation of control distributor concept for a control reconfigurable aircraft', *Proc. AIAA GNC Conf.*, Minneapolis, MN, August 1988, AIAA-88-4139-CP.

14. Buffington, J. M., 'Tailless aircraft control allocation', *Proc. AIAA GNC Conf.*, New Orleans, LA, August 1997, AIAA-97-3605.
15. Isidori, A., *Nonlinear control systems*, 2nd edn., Springer, New York, 1989.
16. 'Multivariable design guidelines', *First Draft*, Honeywell Technology Center, Minneapolis, MN (for Air Force), 18 May 1995.
17. Bugajski, D. J., D. F. Enns and M. R. Elgersma, 'A dynamic inversion based control law with application to the high angle of attack research vehicle', *Proc. AIAA GNC Conf.*, Portland, OR, August 1990, pp. 808–825
18. Brinker, J. S. and K. A. Wise, 'Reconfigurable flight control for a tailless advanced fighter aircraft', *Proc. AIAA GNC Conf.*, Boston, MA, August 1998, Paper # AIAA-98-4107.
19. '*RESTORE System Design Report*', 1st Draft, Boeing -Phantom Works, Jan 1998.
20. Calise A. J., S. Lee, M. Sharma, 'Direct adaptive reconfigurable control of a tailless advanced fighter aircraft', *Proc. AIAA GNC Conf.*, Boston, MA, August 1998, AIAA-98-4108.
21. Enns, D. F, 'Control allocation approaches', *Proc. AIAA GNC Conf.*, Boston, MA, August 1998, AIAA-98-4109.
22. Elgersma, M. R., D. F. Enns and P. Voulgaris, 'Parameter identification for systems with redundant actuators', *Proc. AIAA GNC Conf.*, Boston, MA, August 1998, AIAA-98-4110.

